ELSEVIER

Physica C 363 (2001) 67–74

PHYSICA C

www.elsevier.com/locate/physc

Effects of columnar and point defects on magnetic hysteresis curves produced by three-dimensional vortices in layered superconductors

C.J. Olson [a,*], F. Nori [b]

[a] *Theoretical and Applied Physics Divisions, Los Alamos National Laboratory, Los Alamos, NM 87545, USA*
[b] *Department of Physics, Center for Theoretical Physics, The University of Michigan, Ann Arbor, MI 48109-1120, USA*

Received 24 October 2000; received in revised form 2 April 2001; accepted 10 April 2001

Abstract

Using parallel three-dimensional molecular dynamics simulations of line-like coupled pancake vortices, we consider the effect of inter-layer coupling strength and pinning correlation on the magnetization curves of anisotropic superconductors. Columnar pins produce the largest critical current and are insensitive to layer interaction strength. Point pins are increasingly effective at pinning the vortices as the inter-layer interaction strength drops. © 2001 Elsevier Science B.V. All rights reserved.

PACS: 74.60.Ge; 74.60.Jg

1. Introduction

In bulk isotropic superconductors at low temperatures, vortices can be accurately modeled as perfectly rigid rods aligned with the externally applied magnetic field [1,2]. In an anisotropic material, such as the layered superconductor $Bi_2Sr_2CaCu_2O_x$, at high enough temperatures the vortices no longer appear rigid but are instead broken up into disk-like "pancake vortices", one per layer, with an attractive interaction between pancakes in adjacent layers along the length of the vortex [3–10]. In this case, the fully three-dimensional nature of the vortex must be taken into account when studying the interaction of vortices and pinning sites. An understanding of layered materials is important because many high-temperature superconductors have a layered structure, including $YBa_2Cu_3O_{7-\delta}$ [11–19], $Bi_2Sr_2CaCu_2O_x$ [20,21], and Tl-cuprate superconductors [22–24]. The degree of anisotropy in these materials varies, causing the three-dimensional nature of the vortex to be of greater or lesser importance. In each case, however, the two-dimensional approximation for the flux line used in the simulations described in [1,2] is inadequate.

The interactions between vortices and different types of pinning centers, and the resulting effect on the critical current of the anisotropic material, is not yet completely understood. Artificially created

* Corresponding author. Address: Los Alamos National Laboratory, T-12, MS B268, Los Alamos, NM 87545. Tel.: +1-505-665-1134; fax: +1-505-665-3909.
E-mail address: olson@t12.lanl.gov (C.J. Olson).

0921-4534/01/$ - see front matter
PII: S0921-4534(01)00611-6

pins, such as point or columnar pins, strongly affect the vortex behavior and can further enhance the critical currents, so there is great interest in determining the optimum configuration of artificial pinning. It is still not experimentally possible to directly probe the behavior of pancake vortices in a layered material, although considerable advances in vortex imaging have led to an improved understanding of vortex motion in thin films [25–33].

2. Simulation

Molecular dynamics (MD) simulations can provide insight into the dynamical interaction of vortices and pinning sites. The only three-dimensional MD simulations that have been reported consider either static properties of the vortex lattice, including the melting transition [34,35] and the vortex phase diagram [36,37], or dynamic properties under a uniform driving force [38–40]. No studies of experimentally important magnetization properties have been reported. We have therefore developed a parallelized, three-dimensional extension of our two-dimensional simulation (see, e.g., Refs. [41–48]), and have constructed a series of magnetic hysteresis curves that can be compared to experimental measurements.

2.1. Point and columnar defects in anisotropic superconductors

An anisotropic superconductor can be modeled as separate layers containing pancake vortices, where the magnetic field is applied in a direction normal to the layers. Each magnetic flux line is broken into pancake vortices, one per layer, with an attractive inter-layer interaction between pancakes belonging to the same vortex (see Fig. 1). For the form of the inter-layer interaction, we choose a simple spring model. For simplicity, we assume that the only inter-layer interactions are among pancakes belonging to the same vortex, so that pancakes on different layers belonging to different vortices do not interact. The pancakes within a single layer, all of which belong to different vortices, have a repulsive interaction. This model, which does not employ the exact magnetic interactions used in Refs. [37–40], is similar to the model used in Refs. [36].

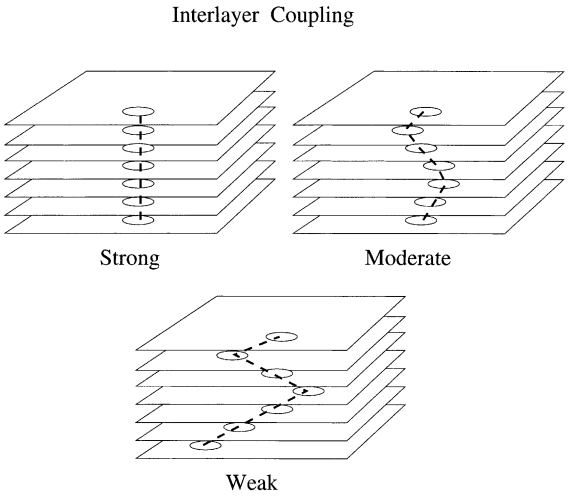

Fig. 1. A single vortex line in an anisotropic superconducting material is broken into a string of pancake vortices, one per layer. Here, the magnetic field is applied normal to the plane of the layers. The coupling between pancakes in different layers varies depending on the degree of anisotropy in the material. Upper left: in a relatively isotropic material, the pancakes are strongly coupled and the vortex line appears as a rigid rod. Upper right: in materials with moderate anisotropy, the vortex line is able to wander transverse to the direction of the applied field. Lower center: in highly anisotropic materials, the coupling between vortices become so weak that the individual pancakes may move independently of each other within their respective layers, and the elastic approximation breaks down.

The overdamped equation of motion for vortex i in layer L is

$$\mathbf{f}_{i,L} = \mathbf{f}_i^{vv} + \mathbf{f}_i^{vI} + \mathbf{f}_i^{vp} = \eta \mathbf{v}_i, \tag{1}$$

where the total force $\mathbf{f}_{i,L}$ on vortex i (due to the other vortices in the same layer $\mathbf{f}_i^{vv}$, pancakes belonging to the same vortex in adjacent layers $\mathbf{f}_i^{vI}$, and pinning sites in the same layer $\mathbf{f}_i^{vp}$) is given by

$$\begin{aligned}\mathbf{f}_{i,L} = & \sum_{j=1}^{N_v} f_0 K_1\left(\frac{|\mathbf{r}_{i,L} - \mathbf{r}_{j,L}|}{\lambda}\right)\hat{\mathbf{r}}_{ij,L} \\ & + \sum_{k=1}^{N_{p,L}} \frac{f_p}{\xi_p}|\mathbf{r}_{i,L} - \mathbf{r}_{k,L}^{(p)}|\Theta\left(\frac{\xi_p - |\mathbf{r}_{i,L} - \mathbf{r}_{k,L}^{(p)}|}{\lambda}\right)\hat{\mathbf{r}}_{ik,L} \\ & + A_{int} f_0(|\mathbf{r}_{i,L} - \mathbf{r}_{i,L-1}|\hat{\mathbf{r}}_{ii\mathrm{d}} + |\mathbf{r}_{i,L} - \mathbf{r}_{i,L+1}|\hat{\mathbf{r}}_{ii\mathrm{u}}).\end{aligned}$$

Here, Θ is the Heaviside step function, K_1 is a modified Bessel function, λ is the penetration depth, $\mathbf{r}_{i,L}$ is the location of the ith vortex in layer L, $\mathbf{v}_{i,L}$ is the velocity of the ith vortex in layer L, $\mathbf{r}^{(\mathrm{p})}_{k,L}$ is the location of the kth pinning site in layer L, ξ_{p} is the pinning site radius, f_{p} is the maximum pinning force, A_{int} is the strength of the inter-layer interaction along a single vortex line, $N_{\mathrm{p},L}$ is the number of pinning sites in layer L, N_v is the number of vortices, and the force is measured in units of

$$f_0 = \frac{\Phi_0^2}{8\pi^2\lambda^3}. \tag{2}$$

For a given layer L, the vortex–vortex unit vectors and the vortex–pinning unit vectors are, respectively, given by

$$\hat{\mathbf{r}}_{ij,L} = \frac{\mathbf{r}_{i,L} - \mathbf{r}_{j,L}}{|\mathbf{r}_{i,L} - \mathbf{r}_{j,L}|}, \qquad \hat{\mathbf{r}}_{ik,L} = \frac{\mathbf{r}_{i,L} - \mathbf{r}^{(\mathrm{p})}_{k,L}}{|\mathbf{r}_{i,L} - \mathbf{r}^{(\mathrm{p})}_{k,L}|}. \tag{3}$$

For a given vortex line i, the pancake vortex in layer L is coupled to the following adjacent pancake vortices: one in layer $L-1$, along $\hat{\mathbf{r}}_{i\mathrm{d}}$, (d for "down"), and one in layer $L+1$, along $\hat{\mathbf{r}}_{i\mathrm{u}}$, (u for "up"). These are given, respectively, by

$$\hat{\mathbf{r}}_{i\mathrm{d}} = \frac{\mathbf{r}_{i,L} - \mathbf{r}_{i,L-1}}{|\mathbf{r}_{i,L} - \mathbf{r}_{i,L-1}|}, \qquad \hat{\mathbf{r}}_{i\mathrm{u}} = \frac{\mathbf{r}_{i,L} - \mathbf{r}_{i,L+1}}{|\mathbf{r}_{i,L} - \mathbf{r}_{i,L+1}|}. \tag{4}$$

We take the pinning force to be $f_{\mathrm{p}} = 0.55 f_0$, the pinning density to be $n_{\mathrm{p}} = 4/\lambda^2$, and the radius of the pinning sites to be $\xi_{\mathrm{p}} = 0.12\lambda$. We consider either strong or moderate inter-layer interactions, with $A_{\mathrm{int}} = 2.0$ or $A_{\mathrm{int}} = 0.5$, respectively.

2.2. Parallel processing

Our sample is composed of N layers, where N ranges from 4 to 24. To handle the large number of pancake vortices in the sample, we use a parallel MD simulation. We divide the system into regions, called domains, which are distributed among the processors. Calculations for each region are carried out simultaneously, and the processors remain coordinated by regular communications using the Message Passing Interface [49] protocol.

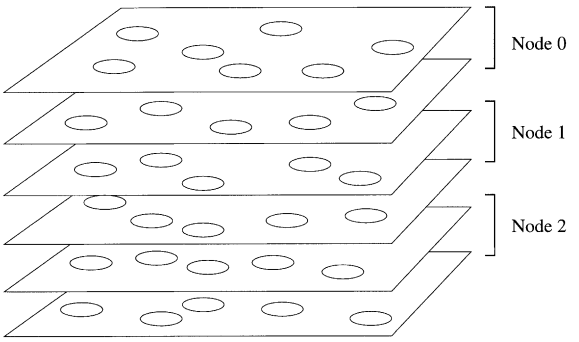

Fig. 2. The one-dimensional domain decomposition used in parallelizing the simulation. The sample is broken into groups of layers. Here, groups of two layers are shown. Each group is assigned to a node. Each node communicates with the two nodes responsible for the layers immediately above and below its domain. We use open boundary conditions in the direction normal to the layers, so the two nodes responsible for the top and bottom of the sample (nodes 0 and 2 in this case) communicate with only one other node.

In our simulation, the domain decomposition is one-dimensional, as shown in Fig. 2. We break the sample into groups of layers, and assign each group to a processor (referred to as "nodes" on the IBM SP2 machine). Each node communicates with the two nodes containing the layers immediately above and below its domain. We use open boundary conditions in the direction normal to the layers, so the two nodes responsible for the top and bottom of the sample communicate with only one other node.

As the simulation runs, each node calculates the repulsive intra-layer interactions of the vortices for every layer it contains. It then finds the inter-layer interactions among the layers for which it is responsible. The nodes then message-pass the positions of the vortices in their end-most layers to the neighboring nodes, so that calculations of interactions between layers on different nodes can be performed.

The straightforward one-dimensional domain decomposition that we use here is ideal for this system. Since there are an equal number of vortices on each layer, load balancing is automatically achieved, meaning that each node must perform the same number of calculations for each MD time step, so no single node can get ahead or behind the

others. The only limitation on the number of layers each node can contain is processor memory. On the IBM SP2 machine that we used, the processors could accommodate up to six layers each. The overall number of layers in the sample is in principle limited only by the number of nodes contained in the machine. We typically used eight nodes for the results presented here.

2.3. Sample geometry

In order to generate magnetic hysteresis curves, we use a sample geometry corresponding to a slab of anisotropic superconductor in a magnetic field applied parallel to the slab surface [50]. The system is periodic in the plane parallel to the applied field. The actual sample region is heavily pinned, and extends from position $x = 4\lambda$ to 20λ. Outside the sample itself is a region with no pinning which extends from $x = 0\lambda$ to 4λ and from $x = 20\lambda$ to 24λ (with $24\lambda = 0\lambda$ according to our periodic boundary conditions). A schematic diagram of the top view of this sample geometry is shown in Fig. 3.

3. Magnetization $M(H)$ curves

We simulate the ramping of an external field H by the slow addition of flux lines to the outside unpinned region. Because there is no pinning in this region, the flux lines attain a fairly uniform density, and we may define the applied field H as Φ_0 times this density. Flux lines from the external region enter the sample through points at the sample edge where the local energy is low. Thus, our simulation models the real situation where vortices nucleate at such low-energy regions at the surface. An image of the vortices in our simulation is shown in Fig. 4. Experimentally, what is typically measured is the average magnetization over the sample volume. In our simulation, we calculate the average magnetization

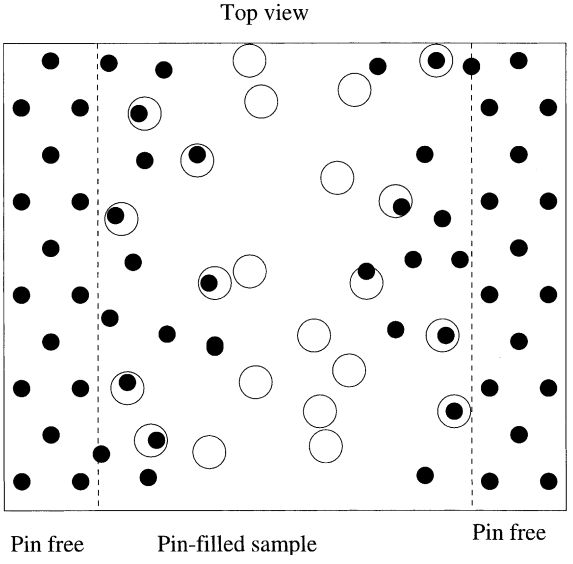

Fig. 3. Schematic top view (looking down on a single layer) of the sample geometry. The sample region is the pinned area in the center of the figure, where pins are represented by large open circles. At the edges of the sample is an unpinned region. Vortices in this area simulate the externally applied magnetic field. To construct a hysteresis loop, vortices are gradually added to the unpinned region. The flux lines enter the sample due to their own mutual repulsion and are trapped by pinning sites.

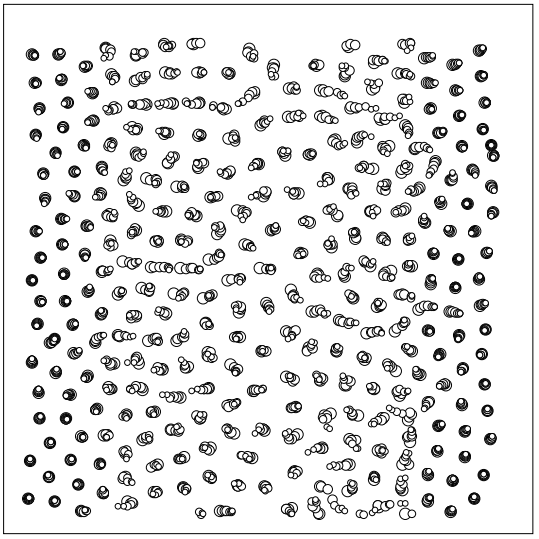

Fig. 4. Vortex positions from a three-dimensional simulation. Circles of a given radius indicate pancake vortices in a given layer, with the largest circles falling in the lowest layer. The external field region appears as an area of evenly spaced vortices aligned with the magnetic field direction. Inside the sample, the moderately coupled pancake vortices bend as they interact with point pinning sites.

$$M = \frac{1}{4\pi V}\int (H - B)\,\mathrm{d}V, \tag{5}$$

as a function of applied field for different pinning parameters.

3.1. Columnar pinning

We first consider samples containing columnar pins, which are modeled as a correlated line of parabolic traps, one in each layer of the sample. If the magnetic field direction is aligned with the columnar pins, then we expect the vortices to behave as perfectly rigid rods. That is, the case of columnar pins can be accurately represented by a two-dimensional simulation. We should therefore observe behavior consistent with an effectively two-dimensional system [50]. As shown in Fig. 5 for a sample containing 16 layers, we find that the width of the hysteresis loop is not affected when the inter-layer interaction force constant A_{int} is changed from moderate coupling, $A_{\mathrm{int}} = 0.5$, to strong coupling, $A_{\mathrm{int}} = 2.0$. This indicates that the three-dimensional character of the vortex line does not play a role in the vortex–pin interactions. Since columnar pins are able to pin a flux line along its entire length without requiring the vortex to bend transverse to the field direction [51], allowing the vortex freedom to flex along its length does not change the ability of a columnar pin to trap a vortex. Thus, in this case we observe effectively two-dimensional behavior.

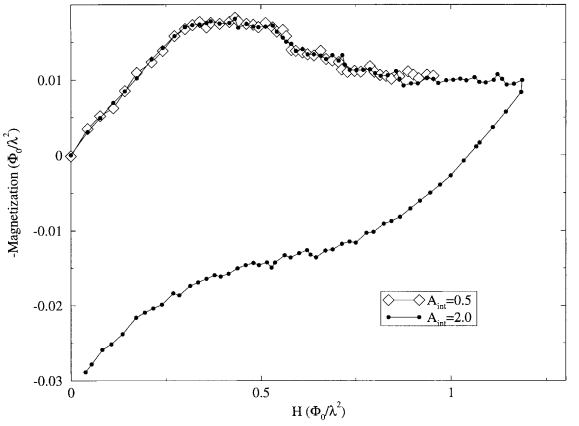

Fig. 5. Magnetization curves for a sample with 16 layers containing columnar pins. The same magnetization behavior is observed regardless of whether the inter-layer vortex interaction is moderate ($A_{\mathrm{int}} = 0.5$, large open diamonds) or strong ($A_{\mathrm{int}} = 2.0$, small filled diamonds).

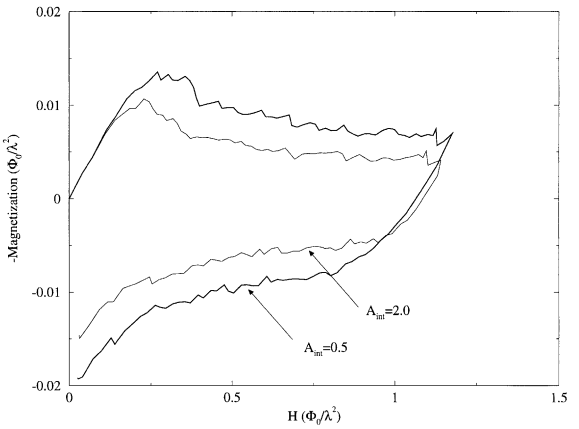

Fig. 6. Magnetization curves for a sample with 16 layers containing randomly located point pins. Larger magnetization is observed when the inter-layer vortex interaction is moderate ($A_{\mathrm{int}} = 0.5$, outer curve) than when it is strong ($A_{\mathrm{int}} = 2.0$, inner curve), indicating that the three-dimensional nature of the vortices is important in this case.

3.2. Point defects

If the pinning sites in the sample are not correlated, but are instead randomly scattered through the sample as point pins, such as those created by proton irradiation [53,54], then the three-dimensional nature of the vortices becomes very important. We can see this in the case of Fig. 6, where hysteresis curves from samples with 16 layers containing random point pinning are shown. If the inter-layer interaction is moderate, an individual vortex line is able to bend significantly in order to take better advantage of the existing pinning and be trapped by as many pinning sites as possible. When the inter-layer interaction strength is increased and the flux lines become correspondingly stiffer, individual vortices can no longer bend enough to intersect a large number of pinning sites. The effective pinning force on the stiff vortices is thus weaker than for the flexible vortices, so the amount of hysteresis is reduced. This shows that the character of the vortices in the third dimension cannot be neglected in a sample containing point pinning.

3.3. Discussion

In actual superconducting materials, point pins occur naturally due to crystalline defects that form during production of the sample. Columnar pins must be added artificially by irradiating the sample with heavy ions [51,54] or neutrons [52]. In experiments, it has been shown that the addition of columnar defects significantly increases the width of the magnetization curve, indicating that such irradiated samples have more desirable vortex pinning characteristics. With our three-dimensional simulation, we can compare the effects of point pins versus columnar pins on the magnetization curve. In Fig. 7, hysteresis curves for two samples with 16 layers and stiff vortices are shown. Both samples contain the same number of pinning sites, but in one sample the pins are spatially uncorrelated, while in the other the pins are aligned into columns parallel with the applied magnetic field. We see that the magnetization is significantly enhanced when the pinning sites are columnar, in good agreement with experimental results [55–57].

Columnar pins are only effective at increasing the critical current when the magnetic field is aligned with the columnar pins. As the alignment is destroyed, the enhancement of pinning is reduced. In Fig. 8, we show the results of tilting the magnetic field direction with respect to the columnar pins in a sample containing eight layers and flexible vortices. Rather than tilting the field lines in our simulation, we tilt the columnar pins by displacing each pin a distance α in a specified direction relative to the pin in the layer above. As seen in Fig. 8, tilting the field away from the pins results in a loss of magnetization enhancement at low applied fields.

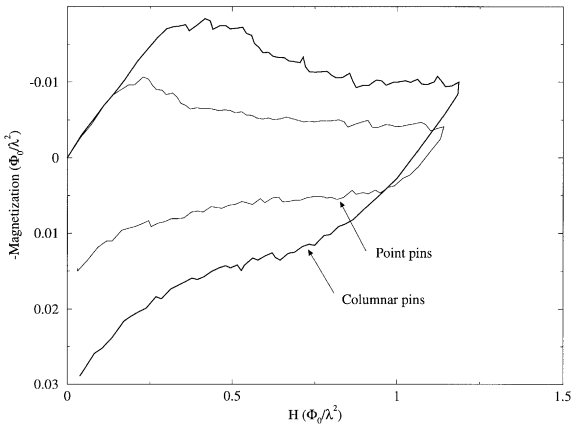

Fig. 7. Magnetization curves for two samples with 16 layers containing stiff vortices ($A_{\text{int}} = 2.0$) and an equal number of pinning sites. In one sample, the point pins are arranged randomly, while in the other sample, columnar pins are present. The sample containing columnar pins produces a much larger magnetization.

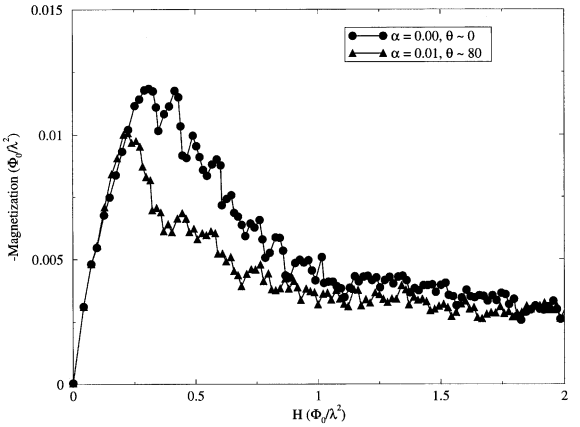

Fig. 8. Magnetization curves for samples with 8 layers containing flexible vortices ($A_{\text{int}} = 0.5$) and columnar pinning sites. The columnar pins are tilted with respect to the applied magnetic field by offsetting each pin a distance α from the pin in the layer above. The offsets used are: $\alpha = 0.0\lambda$ (filled circles), corresponding to a tilt angle of 0°, and $\alpha = 0.10\lambda$ (filled triangles), corresponding to a tilt angle of approximately 80°. The magnetization decreases when the field is tilted away from the direction of the columnar pins.

4. Summary

It is important to take into account the full three-dimensional nature of vortices in anisotropic materials when studying the effects of correlated pinning on the vortex behavior. If pinning sites are regarded as point-like attractive centers scattered among the different layers of the material, then changing the spatial correlation of these sites can affect the vortex behavior.

Our model of vortices as spring-like chains of pancake vortices reproduces expected experimental results: columnar pinning is more effective than

point pinning, but only when the field is aligned with the defects. The effects of tilting the field are also in agreement with experiments. The three-dimensional parallel simulation described here will be useful in studying the dynamics of vortices interacting with a wide array of samples. If the model described here is extended to allow vortex cutting, it will be possible to carry out careful studies of numerous topics of current interest, including entangled vortex phases [58] and flux transformer geometries [59,60].

Several extensions of these studies are possible. For instance, it would be of interest to extend these studies to superconducting samples with periodic arrays of columnar defects (e.g., Refs. [61–70]), which show commensurability effects in $M(H)$. These samples can reach much higher critical currents than the ones with random arrays of pinning sites, and thus are of potential technical importance.

Acknowledgements

We thank J. Clem, H. Marshall, and C. Reichhardt for helpful discussions. We acknowledge the hospitality of the Materials Science Division of Argonne National Laboratory, and partial support under DOE contract no. W-31-109-ENG-38. FN acknowledges partial support from the Center for the Study of Complex Systems and the Michigan Center for Theoretical Physics at The University of Michigan. This is preprint no. MCTP-00-05. CJO acknowledges support from the GSRP of the microgravity division of NASA. Computing services were provided by the Maui High Performance Computing Center, sponsored in part by grant no. F29601-93-2-0001, and by the University of Michigan Center of Parallel Computing, partially funded by NSF grant no. CDA-92-14296.

References

[1] C.J. Olson, C. Reichhardt, F. Nori, Phys. Rev. Lett. 81 (1998) 3757.
[2] C.J. Olson, C. Reichhardt, F. Nori, Phys. Rev. Lett. 80 (1998) 2197.
[3] J.R. Clem, Phys. Rev. B 43 (1991) 7837.
[4] M. Benkraouda, J.R. Clem, Phys. Rev. B 53 (1996) 438.
[5] A. Gurevich, M. Benkraouda, J.R. Clem, Phys. Rev. B 54 (1996) 13196.
[6] J.R. Clem, T. Pe, M. Benkraouda, Physica C 282–287 (1997) 311.
[7] R.G. Mints, I.B. Shapiro, E.H. Brandt, Phys. Rev. B 54 (1996) 9458.
[8] L.N. Bulaevskii, J.R. Clem, L.I. Glazman, Phys. Rev. B 46 (1992) 350.
[9] J.R. Clem, M.W. Coffey, Phys. Rev. B 42 (1990) 6209.
[10] E.H. Brandt, Rep. Prog. Phys. 58 (1995) 1465.
[11] S.Y. Dong, H.S. Kwok, Phys. Rev. B 48 (1993) 6488.
[12] W.K. Kwok et al., Phys. Rev. Lett. 84 (2000) 3706.
[13] W.K. Kwok et al., Phys. Rev. Lett. 80 (1998) 600.
[14] W.K. Kwok et al., Phys. Rev. Lett. 76 (1996) 4596.
[15] W.K. Kwok et al., Phys. Rev. Lett. 73 (1994) 2614.
[16] W.K. Kwok et al., Phys. Rev. Lett. 72 (1994) 1088.
[17] W.K. Kwok et al., Phys. Rev. B 58 (1998) 14594.
[18] U. Welp et al., Phys. Rev. Lett. 76 (1996) 4809.
[19] M.C. Marchetti, D.R. Nelson, Phys. Rev. B 42 (1990) 9938.
[20] S. Sengupta, D. Shi, S. Sergeenkov, P.J. McGinn, Phys. Rev. B 48 (1993) 6736.
[21] U.C. Tauber, H. Dai, D.R. Nelson, C.M. Lieber, Phys. Rev. Lett. 74 (1995) 5132.
[22] E.R. Nowak et al., Phys. Rev. B 54 (1996) 12725.
[23] F. Zuo, S. Khizroev, G.C. Alexandrakis, V.N. Kopylov, Phys. Rev. B 52 (1995) R755.
[24] K.E. Gray, J.D. Hettinger, D.J. Miller, B.R. Washburn, C. Moreau, C. Lee, B.G. Glagola, M.M. Eddy, Phys. Rev. B 54 (1996) 3622.
[25] A. Tonomura, Physica B 280 (2000) 227.
[26] A. Tonomura, Mater. Charact. 42 (1999) 201.
[27] A. Tonomura, Micron 30 (1999) 479.
[28] A. Tonomura, Phys. Scripta T76 (1998) 16.
[29] A. Tonomura et al., Nature 6717 (1999) 308.
[30] C.H. Sow et al., Phys. Rev. Lett. 60 (1998) 2693.
[31] N. Osakabe et al., Phys. Rev. Lett. 78 (1997) 1711.
[32] J. Bonevich et al., Phys. Rev. B 57 (1998) 1200.
[33] K. Harada, O. Kamimura, H. Kasai, F. Matsuda, A. Tonomura, V.V. Moschalkov, Science 274 (1996) 1167.
[34] N.K. Wilkin, H.J. Jensen, Phys. Rev. Lett. 79 (1997) 4254.
[35] N.K. Wilkin, H.J. Jensen, Europhys. Lett. 40 (1997) 423.
[36] A. van Otterlo, R.T. Scalettar, G.T. Zimányi, Phys. Rev. Lett. 81 (1998) 1497.
[37] C.J. Olson, C. Reichhardt, R.T. Scalettar, G.T. Zimányi, N. Grønbech-Jensen, cond-mat/0008350.
[38] C.J. Olson, G.T. Zimányi, A.B. Kolton, N. Grønbech-Jensen, Phys. Rev. Lett. 85 (2000) 5416.
[39] A.B. Kolton, D. Dominguez, C.J. Olson, N. Grønbech-Jensen, Phys. Rev. B 62 (2000) R14657.
[40] C.J. Olson, C. Reichhardt, R.T. Scalettar, G.T. Zimányi, N. Grønbech-Jensen, cond-mat/0006172.
[41] C. Reichhardt, C.J. Olson, J. Groth, S. Field, F. Nori, Phys. Rev. B 53 (1996) R8898.

[42] C.J. Olson, C. Reichhardt, J. Groth, S. Field, F. Nori, Physica C 290 (1997) 89.
[43] C.J. Olson, C. Reichhardt, F. Nori, Phys. Rev. B 56 (1997) 6175.
[44] C.J. Olson, C. Reichhardt, F. Nori, Phys. Rev. Lett. 81 (1998) 3757.
[45] C. Reichhardt, C.J. Olson, F. Nori, Phys. Rev. B 61 (2000) 3665.
[46] J.F. Wambaugh, C. Reichhardt, C.J. Olson, F. Marchesoni, F. Nori, Phys. Rev. Lett. 83 (1999) 5106.
[47] A.P. Mehta, C. Reichhardt, C.J. Olson, F. Nori, Phys. Rev. Lett. 82 (1999) 3641.
[48] J. Groth, C. Reichhardt, C.J. Olson, S. Field, F. Nori, Phys. Rev. Lett. 77 (1996) 3625.
[49] W. Gropp, E. Lusk, A. Skjellum, Using MPI, MIT Press, Cambridge, Mass., 1994.
[50] C. Reichhardt, C.J. Olson, J. Groth, S. Field, F. Nori, Phys. Rev. B 52 (1995) 10441.
[51] L. Civale, Supercond. Sci. Technol. 10 (1997) A11.
[52] F.M. Sauerzopf, H.P. Wiesinger, W. Kritscha, H.W. Weber, G.W. Crabtree, J.Z. Liu, Phys. Rev. B 43 (1991) 3091.
[53] L. Civale, A.D. Marwick, M.W. McElfresh, T.K. Worthington, A.P. Malozemoff, F.H. Holtzberg, J.R. Thompson, M.A. Kirk, Phys. Rev. Lett. 65 (1990) 1164.
[54] L. Civale, M.W. McElfresh, A.D. Marwick, F. Holtzberg, C. Feild, J.R. Thompson, D.K. Christen, Phys. Rev. B 43 (1991) 13732.
[55] M. Konczykowski, F. Rullier-Ablenque, E.R. Yacoby, A. Shaulov, Y. Yeshurun, P. Lejay, Phys. Rev. B 44 (1991) 7167.
[56] L. Civale, A.D. Marwick, T.K. Worthington, M.A. Kirk, J.R. Thompson, L. Krusin-Elbaum, Y. Sun, J.R. Clem, F. Holtzberg, Phys. Rev. Lett. 67 (1991) 648.
[57] A. Umezawa, G.W. Crabtree, J.Z. Liu, H.W. Weber, W.K. Kwok, L.H. Nunez, T.J. Moran, C.H. Sowers, H. Claus, Phys. Rev. B 36 (1987) 7151.
[58] G. Blatter, M.V. Feigel'man, V.B. Geshkenbein, A.I. Larkin, V.M. Vinokur, Rev. Mod. Phys. 66 (1994) 1125.
[59] D. Lopez, E.F. Righi, G. Nieva, F. de la Cruz, W.K. Kwok, J.A. Fendrich, G.W. Crabtree, L. Paulius, Phys. Rev. B 53 (1996) R8895.
[60] D. Lopez, E.F. Righi, G. Nieva, F. de la Cruz, Phys. Rev. Lett. 76 (1996) 4034.
[61] F. Nori, Science 278 (1996) 1373.
[62] T. Matsuda et al., Science 278 (1996) 1393.
[63] K. Harada et al., Science 274 (1996) 1167.
[64] C. Reichhardt, C.J. Olson, J. Groth, S. Field, F. Nori, Phys. Rev. B 54 (1996) 16108.
[65] C. Reichhardt, C.J. Olson, J. Groth, S. Field, F. Nori, Phys. Rev. B 56 (1997) 14196.
[66] C. Reichhardt, C.J. Olson, F. Nori, Phys. Rev. B 58 (1998) 6534.
[67] C. Reichhardt, C.J. Olson, F. Nori, Phys. Rev. B 57 (1998) 7937.
[68] C. Reichhardt, C.J. Olson, F. Nori, Phys. Rev. Lett. 78 (1997) 2648.
[69] C. Reichhardt, F. Nori, Phys. Rev. Lett. 82 (1999) 414.
[70] F. Nori, C. Reichhardt, Physica C 332 (2000) 40.